Research Square

Preprints are preliminary reports that have not undergone peer review.
They should not be considered conclusive, used to inform clinical practice,
or referenced by the media as validated information.

Age-Stratified Hybrid Thresholds for Plasma P-tau 217 in Alzheimer Disease Triage

Pengcheng Li

pengchengli@hainanu.edu.cn

Huazhong University of Science and Technology

Junjie Zhuo

Hainan University https://orcid.org/0000-0002-2764-2690

Junsheng Xu

Hainan University

Zhanbo Zhang

Hainan University

Jiayi Ding

Xuanwu Hospital of Capital Medical University

Hao Wang

State Key Laboratory of Digital Medical Engineering, Key Laboratory of Biomedical Engineering of Hainan Province, School of Biomedical Engineering https://orcid.org/0000-0002-8201-8006

Ying Han

Department of Neurology, Xuanwu Hospital of Capital Medical University

Article

Keywords:

Posted Date: November 26th, 2026

DOI: https://doi.org/10.21203/rs.3.rs-11522715/v1

License: This work is licensed under a Creative Commons Attribution 4.0 International License.
Read Full License

Additional Declarations:
There is **NO** Competing Interest.

A statement of ethics approval – This study is a secondary analysis of de-identified, publicly available data obtained from the Alzheimer's Disease Neuroimaging Initiative (ADNI) , the Health & Aging Brain

Study-Health Disparities (HABS-HD), and the Anti-Amyloid Treatment in Asymptomatic Alzheimer's (A4)/Longitudinal Evaluation of Amyloid Risk and Neurodegeneration (LEARN) studies, accessed under their respective data use agreements. The SILCODE (ClinicalTrials.gov identifier: NCT03370744) study was approved by the Ethics Committee of Xuanwu Hospital of Capital Medical University (2017[046]). A statement on participant consent - All participants provided written informed consent.

Age-Stratified Hybrid Thresholds for Plasma P-tau 217 in Alzheimer Disease Triage

Junjie Zhuo[1]; Junsheng Xu[1]; Zhanbo Zhang[1]; Jiayi Ding[2]; Hao Wang[1]; Yin Han[1,2,3,4#]; Pengcheng Li[1#]; for the Alzheimer's Disease Neuroimaging Initiative*, Anti-Amyloid Treatment in Asymptomatic Alzheimer's and Longitudinal Evaluation of Amyloid Risk and Neurodegeneration (A4 and LEARN) studies, and Health & Aging Brain Study–Health Disparities (HABS-HD)

1. State Key Laboratory of Digital Medical Engineering, Key Laboratory of Biomedical Engineering of Hainan Province, School of Biomedical Engineering, Hainan University, Sanya. 572025;

2. Department of Neurology, Xuanwu Hospital of Capital Medical University, Beijing, 100053;

3. Department of Neurology of the Affiliated Hospital of Hangzhou Normal University, Hangzhou, 310015;

4. Department of Geriatrics of Changji People's Hospital, Changji, 831100.

 # Yin Han and Pengcheng Li are the corresponding authors, Correspondence Address: hanying@xwh.ccmu.edu.cn; pengchengli@hainanu.edu.cn

** Data used in preparation of this article were obtained from the Alzheimer's Disease Neuroimaging Initiative (ADNI) database (adni.loni.usc.edu). As such, the investigators within the ADNI contributed to the design and implementation of ADNI and/or provided data but did not participate in analysis or writing of this report. A complete listing of ADNI investigators can be found at: http://adni.loni.usc.edu/wp-content/uploads/how_to_apply/ADNI_Acknowledgement_List.pdf*

Abstract

Blood-based biomarkers, particularly plasma phosphorylated tau 217 p-tau217, are transforming Alzheimer's disease (AD) diagnosis. However, current diagnostic workflows utilizing universal global cutoffs are profoundly confounded by age-related physiological elevations in p-tau217, frequently yielding unmanageably large indeterminate "grey" zones. Here, utilizing longitudinal and cross-sectional data from 4,048 participants across four independent cohorts, we characterize the age-dependent biological trajectory of p-tau217 and propose a tailored diagnostic framework. We identified a critical temporal inflection point at 74 years of age. In amyloid-β-positive individuals aged 74 years and older, p-tau217 concentrations reach a biological plateau, approximating those of patients with symptomatic AD and substantially diminishing discriminative accuracy (AUC < 0.70). To address this age-driven biological drift, we developed an age-stratified hybrid threshold strategy. Compared with standard global double cutoffs, this hybrid approach reduced the proportion of indeterminate results requiring confirmatory positron emission tomography by more than 50%. The strategy achieved the highest diagnostic specificity across cohorts, substantially improving positive predictive values (74% to 96%) while preserving high overall diagnostic accuracy (80% to 89%). Furthermore, health economic modeling demonstrated that this framework minimizes unnecessary confirmatory testing and unwarranted treatments, saving up to $1.17 million per 1,000 screened patients. Ultimately, physiological aging independently dictates p-tau217 trajectories, necessitating age-adjusted clinical decision limits to establish a scalable, highly specific, and cost-effective triage pathway for AD.

Introduction

The clinical management of Alzheimer disease (AD) is evolving with the introduction of disease-modifying therapies targeting amyloid-β (Aβ) pathology[1,2]. Early intervention is critical for therapeutic efficacy, elevating population-level screening to a global public health priority amid the escalating dementia burden[3,4]. Compared with expensive and invasive positron emission tomography (PET) or cerebrospinal fluid (CSF) testing, plasma phosphorylated tau 217 (p-tau217) has emerged as a highly accurate, cost-effective, and scalable alternative for detecting AD pathology[5-7] and predicting future cognitive decline[8,9]. However, translating this analytical performance into clinical practice requires carefully defined diagnostic thresholds[10-12].

Current consensus guidelines advocate a 2-step diagnostic workflow utilizing a global double-cutoff strategy[13], which should ideally limit indeterminate results to 15% to 20% of the tested population[14]. While a recent meta-analysis confirm that plasma p-tau217 robustly detects Aβ pathology even among cognitively unimpaired (CU) older adults[15], other studies demonstrate that plasma p-tau217 levels also increase naturally with physiological aging[16] and medical comorbidities[17,18]. Applying a uniform global cutoff fails to account for these physiological variations, thereby introducing differential misclassification across age groups[19]. As a result, the proportion of individuals classified into the intermediate zone frequently exceeds recommended thresholds, particularly among older adults[10,20]. This high rate of indeterminate results requires additional confirmatory testing, which compromises the cost-effectiveness of blood-based screening and strains healthcare resources[14,21].

To optimize the clinical utility of plasma p-tau217, we analyzed longitudinal and cross-sectional data from 4 independent cohorts (A4 and LEARN, HABS-HD, ADNI, and SILCODE) to identify the age-related inflection point for p-tau217 accumulation. Based on these pathophysiological findings, we developed an age-stratified hybrid threshold strategy to mitigate differential misclassification. This study aimed to evaluate the diagnostic performance and health economic impact of this approach compared with standard global cutoffs. Specifically, we assessed its ability to decrease the proportion of indeterminate results, optimize diagnostic specificity, and meet established consensus criteria for clinical implementation.

Results

Participants

The sample comprised 4048 participants (A4 and LEARN, n = 1582; HABS-HD, n = 1208; ADNI, n = 1068; SILCODE, n = 190). Female participants constituted the majority across all 4 cohorts (A4 and LEARN, 948 [60%]; HABS-HD, 752 [62%]; ADNI, 570 [53%]; and

SILCODE, 115 [61%]). Mean (SD) educational attainment ranged from 13.40 (3.29) years in the SILCODE cohort to 16.62 (2.76) years in the A4 cohort. The mean (SD) age at the first visit ranged from 69.2 (6.3) years in HABS-HD to 74.0 (7.5) years in ADNI; at the last recorded visit, the mean (SD) age advanced to a range of 69.6 (6.3) years to 75.0 (7.6) years across the respective cohorts.

At the first visit, the proportion of CU participants varied by cohort design, being highest in A4 and LEARN (1570 [99%]), followed by SILCODE (156 [82%]), HABS-HD (912 [75%]), and ADNI (605 [57%]). By the last visit, clinical diagnoses had progressed; the prevalence of mild cognitive impairment in the A4 and LEARN cohort increased from 0.8% at baseline to 23%, and dementia prevalence in the ADNI cohort was 12%. Additional baseline and longitudinal characteristics, including amyloid PET positivity rates and plasma p-tau217 concentrations, are detailed in Table 1.

Longitudinal Trajectories of Plasma p-tau217 in CU participants

In the discovery phase (A4 and LEARN), Bayesian modeling identified a temporal inflection point at age 74.45 years for Aβ-positive CU individuals. Prior to age 74.45 years, Aβ-positive participants demonstrated a higher accumulation rate than Aβ-negative participants (slope difference, 0.13 SD units/year; 95% credible interval [CrI], 0.08 to 0.17). After age 74.45 years, p-tau217 accumulation in Aβ-positive individuals plateaued (slope change, −0.05 SD units/year; 95% CrI, −0.14 to 0.06). Aβ-negative participants exhibited no significant temporal inflection point (knot estimate, 5.81; 95% CrI, −0.76 to 11.44). Validation cohorts (HABS-HD and ADNI) confirmed this trajectory, demonstrating sustained accumulation driven by Aβ pathology and age, without significant postinflection acceleration (Figure1).

Cross-Sectional Analysis and Age-Dependent Diagnostic Performance

We evaluated optimal plasma p-tau217 z score thresholds across age utilizing 1-year sliding windows. The optimal diagnostic threshold remained stable prior to age 74 years and increased thereafter, diverging from the global cutoff (eFigure 1 in Supplement 1).

In cross-sectional analyses at the last available visit, plasma p-tau217 concentrations among Aβ–positive CU individuals were significantly higher in participants aged 74 years and older compared with those younger than 74 years across all 4 cohorts (all $P < .01$) (Figure2). Among Aβ-positive symptomatic patients (MCI and dementia), p-tau217 concentrations demonstrated no significant age-related differences in 3 of the 4 cohorts (A4 and LEARN, ADNI, and SILCODE), whereas significant age-related differences were observed in the HABS-HD cohort. Sensitivity analyses utilizing biomarker data from the first visits yielded consistent results for these age-related patterns across cognitive stages (eFigure 2 in Supplement 1).

In ROC analyses (Figure2), plasma p-tau217 maintained high accuracy in differentiating

amyloid-β (Aβ)–positive symptomatic patients from Aβ-negative CU individuals across all age strata (AUC range, 0.89 to 0.96). Conversely, the ability to differentiate Aβ-positive symptomatic patients from Aβ-positive CU individuals was substantially diminished, particularly in the older age group (≥74 years). AUC values utilizing this older demographic as the reference group decreased to 0.71 in the A4 and LEARN cohort, 0.55 in HABS-HD, 0.77 in ADNI, and 0.70 in SILCODE. Statistical comparisons via the DeLong test revealed that this attenuation in AUC between the younger (60 to 74 years) and older (≥74 years) Aβ-positive CU reference groups was significant in the A4 and LEARN (P = .003) and HABS-HD (P = .004) cohorts, with consistent directional trends observed in the ADNI (P = .27) and SILCODE (P = .09) cohorts (eTable 3-6 in Supplement 1). Furthermore, AUCs derived using older Aβ-positive CU individuals were significantly lower than those using Aβ-negative CU individuals across all 4 cohorts (all P < .05). Sensitivity analyses utilizing diagnostic data from the first available visits fully replicated this attenuation of discriminative accuracy in the older age stratum (eFigure 2 in Supplement 1).

Implementation of the Hybrid Strategy and Reduction of the Intermediate Zone

Diagnostic thresholds were applied to the biomarker data from the last recorded visit of each participant (Figure 3, A-D). Evaluations of diagnostic strategies revealed an asymmetrical misclassification pattern driven by age-related elevations in plasma p-tau217 (eFigures 3 and 4 in Supplement 1). Specifically, compared with uniform global thresholds, the application of strictly age-specific cutoffs across both single- and double-threshold methods consistently increased false-positive classifications and decreased false-negative classifications in the <74 years group. Conversely, this age-specific approach decreased false-positive classifications and increased false-negative classifications in the ≥74 years group. To mitigate this differential misclassification, we implemented the age-dependent hybrid threshold strategy (Figure 3E).

Application of the hybrid strategy substantially reduced the proportion of intermediate cases requiring confirmatory amyloid PET testing compared with the standard global double cutoff at the last visit (Figure 3F). In the HABS-HD cohort, the intermediate zone proportion decreased from 56.3% using the global double cutoff to 19.5% using the hybrid strategy (absolute reduction, 36.8%). Consistent reductions were observed in ADNI (from 40.1% to 13.4%; absolute reduction, 26.7%), SILCODE (from 71.1% to 28.4%; absolute reduction, 42.7%), and the A4 and LEARN cohort (from 33.8% to 20.1%; absolute reduction, 13.7%). Similar trends in intermediate zone reductions were maintained when analyses were performed using data from the first visits of participants (eFigure 5 in Supplement 1).

Diagnostic Performance and Health Economic Impact

Comprehensive diagnostic performance metrics at the last visit, excluding cases in the intermediate zone, were evaluated across the 5 threshold strategies (Figure 4A; detailed metrics

are provided in eTable 7 in Supplement 1). Across all cohorts, the hybrid strategy yielded higher specificity and PPV compared with the global and age-specific single-cutoff approaches. For instance, in the HABS-HD cohort, the hybrid strategy improved specificity to 90% (95% CI, 88% to 92%) compared with 84% (95% CI, 82% to 87%) for the global single cutoff, and improved PPV to 74% (95% CI, 69% to 79%) compared with 63% (95% CI, 58% to 68%). Furthermore, the hybrid strategy maintained an overall diagnostic accuracy of 88% (95% CI, 86% to 90%) in the HABS-HD cohort. This accuracy was comparable to the 89% (95% CI, 86% to 92%) accuracy achieved by the global double cutoff, but the hybrid strategy accomplished this while substantially reducing the proportion of indeterminate cases.

In a modeled clinical scenario of 1000 suspected patients at their last visit, the hybrid strategy yielded highly favorable economic profiles (Figure 4B). This economic benefit was particularly evident in the A4 and LEARN cohort, representing a clinical trial screening population. In this cohort, the estimated total cost was $1.91 million using the hybrid strategy, representing a substantial reduction from $2.26 million using the global single cutoff and $2.10 million using the global double cutoff. Similar prominent cost reductions were observed in the HABS-HD and SILCODE cohorts, where the hybrid strategy consistently yielded the lowest overall costs. In the ADNI cohort, the total cost of the hybrid strategy was markedly lower than those of the single-cutoff approaches and comparable to the costs of the double-cutoff strategies.

Discussion

In this multicohort diagnostic study, physiological aging significantly confounded the clinical interpretation of plasma p-tau217. We identified a distinct temporal inflection point at age 74 years for biomarker accumulation. To balance diagnostic accuracy with clinical feasibility, we developed an age-stratified hybrid threshold strategy. Across 4 independent cohorts, this approach reduced the proportion of patients requiring confirmatory PET by more than 50% compared with standard global two-cutoffs, preserved high overall diagnostic accuracy, and yielded a highly favorable health economic profile.

These clinical improvements are rooted in the age-dependent biological trajectory of plasma p-tau217 (Figure1, 2, and eFigure1, 2 in Supplement 1). Extensive autopsy-based studies have long established that the prevalence and severity of AD neuropathologic changes, including amyloid plaques and neurofibrillary tangles, increase ubiquitously with advancing age over several decades[22]. Recent meta-analyses affirm that p-tau217 robustly detects Aβ pathology among CU older adults[15]. Concurrently, community-based studies indicate that p-tau217 concentrations increase naturally with age[16,18,19] and declining kidney function[11,17]. Our longitudinal and cross-sectional analyses clarify that the temporal inflection point at age 74 years is specific to the preclinical phase. Beyond age 74 years, concentrations in Aβ-positive CU individuals approximated those of Aβ-positive symptomatic patients (MCI and dementia).

Consequently, the discriminative accuracy of p-tau217 between Aβ-positive CU and symptomatic patients older than 74 years was poor. This age-driven convergence is consistent with established dynamic models of AD pathophysiology, suggesting that continuous decades of neuropathological accumulation eventually drive p-tau217 to a biological ceiling[23]. This phenomenon provides a mechanistic explanation for recent observations of decreased diagnostic accuracy among the oldest old[19] and indicates that advanced age drives p-tau217 to a physiological upper limit, obscuring the biomarker distinction between preclinical and symptomatic stages.

These biological findings underscore the inherent limitations of applying uniform global cutoffs. Community-based studies demonstrate that distinct biological profiles require tailored thresholds to prevent systematic misclassification[17,18]. Extending this principle to chronological age, our data reveal that uniform or strictly age-specific thresholds inadequately balance sensitivity and specificity, classifying a disproportionate number of individuals into the indeterminate zone, a recognized barrier to scalable screening[10,20].

The hybrid strategy addresses this asymmetrical misclassification by integrating age-stratified rule-in and rule-out bounds. This tailored approach successfully compressed the intermediate zone to 13.4% to 20.1% in the ADNI, HABS-HD, and A4 and LEARN cohorts, aligning with the Global CEO Initiative target of 20% or less[14]. Although the intermediate zone in the SILCODE cohort remained at 28.4%, this represented an absolute reduction of 42.7% compared with the global cutoff. This variation highlights the crucial epidemiological principle that the clinical composition of a cohort fundamentally influences biomarker performance metrics[24]. The exceptionally high proportion of asymptomatic participants in our sample (exceeding 50% even in ADNI) drove differences from highly selected clinical cohorts, mirroring true community-based screening settings[16,18,19]. Furthermore, the ADNI cohort, which possessed the lowest CU proportion, exhibited the smallest intermediate zone (13.4%). These findings demonstrate that diagnostic algorithms validated in advanced clinical settings may artificially yield inflated indeterminate rates when extrapolated to earlier, preclinical populations[25]. The ability of the hybrid strategy to substantially reduce the intermediate zone across these early-stage populations underscores its robust clinical utility.

A central feature of the hybrid strategy is the explicit prioritization of diagnostic specificity to mitigate the risks of false-positive classifications. In the era of anti-amyloid immunotherapies, false-positive diagnoses carry severe consequences, including the risk of amyloid-related imaging abnormalities (ARIA) and the misallocation of resources toward ineffective treatments[26,27]. By optimizing specificity, the hybrid strategy substantially improved positive predictive values (PPVs) compared with global single cutoffs. Although standard double cutoffs yielded marginally higher PPVs by excluding a disproportionately large number of borderline cases from the analysis, the hybrid strategy maintained highly competitive predictive

performance while providing definitive classifications for a substantially larger population. Within the hybrid framework, PPVs reached 87% to 96% in cohorts with higher Aβ prevalence (ADNI and A4 and LEARN) but were moderately lower in the HABS-HD (74%) and SILCODE (82%) cohorts. Despite this prevalence-driven attenuation and the inclusion of more challenging borderline cases, the hybrid strategy consistently provided an optimal balance of high diagnostic specificity and overall accuracy (ranging from 80% to 89%), offering clinicians actionable results in primary care settings lacking confirmatory testing capacity[12,13].

Furthermore, the health economic implications are highly relevant as healthcare systems prepare for widespread disease-modifying therapy rollout amid the escalating global burden of dementia[3,28,29]. Scalable screening requires scalable triage algorithms. Relying on single cutoffs incurs substantial misdiagnosis penalties, whereas standard double cutoffs merely shift the financial burden to radiology departments[21,30]. By reducing confirmatory testing needs, the hybrid strategy offers a pragmatic, cost-saving framework for clinical integration[31].

Strengths and Limitations

Strengths include robust validation across 4 independent cohorts utilizing diverse, highly accurate p-tau217 platforms. However, limitations exist. First, although the A4 and LEARN study represents an international, multicenter phase 3 clinical trial, participants across these Western-based cohorts (including ADNI and HABS-HD) remain predominantly White and highly educated. This relative lack of racial and ethnic diversity may influence biomarker thresholds[32,33], although the inclusion of the SILCODE cohort mitigates this limitation by providing valuable validation in Chinese population. Second, real-world economic costs will vary based on regional healthcare systems. Third, future research must evaluate the longitudinal psychological and behavioral outcomes of disclosing biomarker results based on tailored thresholds[34].

Conclusions

Physiological aging significantly elevates plasma p-tau217 concentrations independently of amyloid pathology, necessitating age-stratified clinical decision limits. The proposed hybrid threshold strategy safely reduced the proportion of patients requiring expensive confirmatory testing while maximizing diagnostic specificity and health economic cost-savings. This approach provides a pragmatic and robust framework for the global implementation of AD blood biomarker screening.

Methods

Study Population

This study analyzed data from 4 independent observational and clinical trial cohorts: the Anti-

Amyloid Treatment in Asymptomatic Alzheimer's study and the companion Longitudinal Evaluation of Amyloid Risk and Neurodegeneration cohort (A4 and LEARN)[35], the Health & Aging Brain Study-Health Disparities (HABS-HD)[36], the Alzheimer's Disease Neuroimaging Initiative (ADNI), and the Sino Longitudinal Study on Cognitive Decline (SILCODE)[37] study (data collected October 2010 to May 2026). Inclusion was restricted to participants aged 60 years and older, encompassing CU individuals and patients with mild cognitive impairment (MCI) or dementia. All participants underwent at least 1 time concurrent plasma p-tau217 and Aβ PET imaging.

Plasma P-tau 217

Plasma p-tau217 was quantified using 3 distinct immunoassay platforms across the 4 cohorts (eTable 2 in Supplement 1). The analytical platforms included the Quanterix Single Molecule Array (Simoa) platform (for SILCODE and HABS-HD), an electrochemiluminescence immunoassay developed by Eli Lilly and Company on the Meso Scale Diagnostics (MSD) platform (for A4 and LEARN), and the fully automated Lumipulse G1200 chemiluminescence immunoassay by Fujirebio (for ADNI). Extreme outliers for plasma p-tau217, defined as values exceeding 3 SDs from the mean, were excluded within each cohort[17].

Aβ PET and Aβ status

Brain amyloid burden was quantified using amyloid PET imaging, with standardized uptake value ratios (SUVRs) calculated using a whole cerebellum reference region across all cohorts. The radiotracers utilized included ^{18}F-florbetapir (A4 and ADNI) and ^{18}F-florbetaben (HABS-HD and ADNI). Aβ positivity was determined as a mean cortical SUVR of 1.15 or greater in the A4 cohort[35] and a global SUVR of 1.08 or greater in the HABS-HD cohort (calculated as the unweighted mean of 4 regional cortical SUVRs)[36]. For the ADNI cohort, Aβ positivity was defined as a cortical summary SUVR of 1.11 or greater for ^{18}F-florbetapir and 1.08 or greater for ^{18}F-florbetaben[38]. For the SILCODE cohort, PET image processing aligned with the ADNI analytical pipeline[38]. Aβ positivity was defined as an SUVR greater than 0.793 (using a composite reference region), an optimal threshold derived by maximizing the Youden index to differentiate patients with AD dementia from CU individuals.

Statistics

Biomarker Harmonization and Longitudinal Modeling

To harmonize biomarker measurements across different cohorts and assays, plasma p-tau217 levels were first standardized into z scores using the mean and SD of the Aβ-negative CU reference group within each respective cohort[39]. Among CU participants, Bayesian piecewise linear mixed-effects models were employed in the discovery cohort (A4 and LEARN) to estimate a data-driven temporal knot for age-related p-tau217 accumulation, adjusting for

repeated measures via random intercepts. This predefined knot was subsequently evaluated in independent validation cohorts (HABS-HD and ADNI) using segmented Bayesian mixed-effects models.

Cross-Sectional Analysis

Cross-sectional analyses utilized data from each participant's last available visit. Participants were stratified by Aβ PET status, clinical diagnosis, and the derived age inflection point (60 to 74 years vs ≥74 years). Pairwise comparisons of log-transformed p-tau217 concentrations were evaluated using analysis of covariance adjusted for sex and education.

Development of the Age-Adjusted Hybrid Threshold Strategy

Global and age-specific single cutoffs were determined via receiver operating characteristic (ROC) analysis maximizing the Youden index. Double cutoffs were established by setting upper and lower bounds to yield 95% specificity and 95% sensitivity, respectively, with 1000 bootstrap resamples. To mitigate age-driven misclassification, we developed an age-adjusted hybrid threshold strategy: for adults aged 60 to 74 years, the age-specific optimal cutoff defined negativity and the upper cutoff defined positivity; for adults aged 74 years and older, the lower cutoff defined negativity and the optimal cutoff defined positivity. Values falling between these bounds constituted the indeterminate zone.

Diagnostic Performance and Sensitivity Analysis

Diagnostic performance metrics, including sensitivity, specificity, positive predictive value (PPV), negative predictive value (NPV), and accuracy, were calculated. For strategies incorporating a double-cutoff or hybrid approach, intermediate cases were assumed to require confirmatory Aβ PET imaging; therefore, these indeterminate cases were excluded from the primary accuracy calculations, and the proportion of intermediate cases was reported separately. Diagnostic accuracies across different strategies were compared using the McNemar test.

Health Economic Impact Analysis

Using established health economic frameworks[17], we calculated the frequencies and associated financial penalties of indeterminate, false-positive, and false-negative classifications. Indeterminate cases were modeled to require confirmatory Aβ PET imaging at an estimated cost of $4000. False-positive classifications incurred a $30,000 penalty. False-negative classifications were assigned an $8000 opportunity cost, reflecting the clinical loss of withholding disease-modifying therapies.

Sensitivity analyses were performed using data from the first available time point for each participant to ensure the robustness of the findings.

All tests were 2-sided with statistical significance set at $P < .05$. Analyses were performed using

R version 4.3.2 (R Foundation) and RStudio version 2026.01.1 + 403 (Posit).

Author Contributions: P.L. and Y.H. supervised the study. J.Z. were responsible for the design of the concept and the study. J.Z., J.X., and Z.Z. contribution to the data analysis; J.Z. and J.X. performed the statistical analysis; H.W., J.D., and Y.H. contributions to the SILCODE dataset analysis, J.Z., J.X., Z.Z., Y.H. and P.L. made substantial contributions to the discussion on the results and the manuscript; J.Z., Y.H. and P.L. wrote the manuscript.

Group Information: A complete list of the members of ADNI, the A4 and LEARN studies, and HABS-HD appears in Supplement2.

Funding/Support: This work was partially supported by the Natural Science Foundation of China (Grant Nos. 82260227, 62527820, and 82327809); First-class Discipline Breakthrough Initiative of Hainan University (XKTP2025B04); the Construction Fund of Key Medical Disciplines of Hangzhou（2025HZGF02）.

Data collection and sharing for this project was funded by the Alzheimer's Disease Neuroimaging Initiative (ADNI) (National Institutes of Health Grant U01 AG024904) and DOD ADNI (Department of Defense award number W81XWH-12-2-0012). ADNI is funded by the National Institute on Aging, the National Institute of Biomedical Imaging and Bioengineering, and through generous contributions from the following: AbbVie, Alzheimer's Association; Alzheimer's Drug Discovery Foundation; Araclon Biotech; BioClinica, Inc.; Biogen; Bristol-Myers Squibb Company; CereSpir, Inc.; Cogstate; Eisai Inc.; Elan Pharmaceuticals, Inc.; Eli Lilly and Company; EuroImmun; F. Hoffmann-La Roche Ltd and its affiliated company Genentech, Inc.; Fujirebio; GE Healthcare; IXICO Ltd.; Janssen Alzheimer Immunotherapy Research & Development, LLC.; Johnson & Johnson Pharmaceutical Research & Development LLC.; Lumosity; Lundbeck; Merck & Co., Inc.; Meso Scale Diagnostics, LLC.; NeuroRx Research; Neurotrack Technologies; Novartis Pharmaceuticals Corporation; Pfizer Inc.; Piramal Imaging; Servier; Takeda Pharmaceutical Company; and Transition Therapeutics. The Canadian Institutes of Health Research is providing funds to support ADNI clinical sites in Canada. Private sector contributions are facilitated by the Foundation for the National Institutes of Health (www.fnih.org). The grantee organization is the Northern California Institute for Research and Education, and the study is coordinated by the Alzheimer's Therapeutic Research Institute at the University of Southern California. ADNI data are disseminated by the Laboratory for Neuro Imaging at the University of Southern California.

HABS-HD was supported by the NIA of the NIH (R01AG054073, R01AG058533, R01AG070862, P41EB015922, U19AG078109).

The A4/LEARN studies were funded by the NIA (U19AG010483, R01AG063689), Eli Lilly,

and several philanthropic organizations. The A4 study is funded by a public-private philanthropic partnership, including funding from the NIH/NIA (U19AG010483, R01AG063689), Eli Lilly, Alzheimer's Association, Accelerating Medicines Partnership, GHR Foundation, an anonymous foundation, and additional private donors, with in-kind support from Avid, Cogstate, Albert Einstein College of Medicine, and Foundation for Neurologic Diseases. The companion observational LEARN study is funded by the Alzheimer's Association and GHR Foundation.

Conflict of interest: The authors declare that they have no competing financial interests.

Acknowledgments: The authors used Gemini and ChatGPT for language editing and manuscript polishing. The authors take full responsibility for the final content.

Reference

1. van Dyck CH, Swanson CJ, Aisen P, et al. Lecanemab in Early Alzheimer's Disease. *New Engl J Med*. 2023;388(1):9–21.
2. Sims JR, Zimmer JA, Evans CD, et al. Donanemab in Early Symptomatic Alzheimer Disease. *JAMA*. 2023;330(6)
3. Nichols E, Steinmetz JD, Vollset SE, et al. Estimation of the global prevalence of dementia in 2019 and forecasted prevalence in 2050: an analysis for the Global Burden of Disease Study 2019. *The Lancet Public Health*. 2022;7(2):e105–e125.
4. Livingston G, Huntley J, Liu KY, et al. Dementia prevention, intervention, and care: 2024 report of the Lancet standing Commission. *The Lancet*. 2024;404(10452):572–628.
5. Palmqvist S, Janelidze S, Quiroz YT, et al. Discriminative Accuracy of Plasma Phospho-tau217 for Alzheimer Disease vs Other Neurodegenerative Disorders. *JAMA*. 2020;324(8)
6. Palmqvist S, Tideman P, Mattsson-Carlgren N, et al. Blood Biomarkers to Detect Alzheimer Disease in Primary Care and Secondary Care. *JAMA*. 2024;332(15)
7. Ashton NJ, Brum WS, Di Molfetta G, et al. Diagnostic Accuracy of a Plasma Phosphorylated Tau 217 Immunoassay for Alzheimer Disease Pathology. *JAMA Neurology*. Mar 2024;81(3):255–263.
8. Buckley RF, Townsend DL, Birkenbihl CJ, et al. Prognostic Value of Blood-Based P-Tau217 Levels for Progression to Cognitive Impairment. *JAMA*. 2026;336(11)
9. Mattsson-Carlgren N, Salvadó G, Ashton NJ, et al. Prediction of Longitudinal Cognitive Decline in Preclinical Alzheimer Disease Using Plasma Biomarkers. *JAMA Neurology*. 2023;80(4)
10. Hazan J, Liu KY, Isaacs JD, Howard R. Cut-points and gray zones: The challenges of integrating Alzheimer's disease plasma biomarkers into clinical practice. *Alzheimer's & Dementia*. 2025;21(3)
11. Zetterberg H, Bendlin BB. Biofluid biomarkers in Alzheimer's disease and other neurodegenerative dementias. *Nature*. 2026;650(8100):49–59.

12. Ossenkoppele R, van der Kant R, Hansson O. Tau biomarkers in Alzheimer's disease: towards implementation in clinical practice and trials. *The Lancet Neurology*. Aug 2022;21(8):726–734.
13. Hansson O, Edelmayer RM, Boxer AL, et al. The Alzheimer's Association appropriate use recommendations for blood biomarkers in Alzheimer's disease. *Alzheimers Dement*. Dec 2022;18(12):2669–2686.
14. Schindler SE, Galasko D, Pereira AC, et al. Acceptable performance of blood biomarker tests of amyloid pathology — recommendations from the Global CEO Initiative on Alzheimer's Disease. *Nature Reviews Neurology*. 2024;20(7):426–439.
15. Malek-Ahmadi M, Sharma S, Stipho F, et al. Plasma Phosphorylated Tau 217 and Amyloid Burden in Older Adults Without Cognitive Impairment. *JAMA Neurology*. 2026;83(1)
16. Aarsland D, Sunde AL, Tovar-Rios DA, et al. Prevalence of Alzheimer's disease pathology in the community. *Nature*. Feb 5 2025;650(8100):182–186.
17. Yun J, Lee J, Shin D, et al. Plasma Phosphorylated Tau 217 Cutoffs for Amyloid Pathology and Kidney Function, Body Mass Index, and Anemia. *JAMA Neurology*. Mar 2026;83(3):269–279.
18. Mielke MM, Dage JL, Frank RD, et al. Performance of plasma phosphorylated tau 181 and 217 in the community. *Nature Medicine*. 2022;28(7):1398–1405.
19. Palmqvist S, Warmenhoven N, Anastasi F, et al. Plasma phospho-tau217 for Alzheimer's disease diagnosis in primary and secondary care using a fully automated platform. *Nature Medicine*. Jun 2025;31(6):2036–2043.
20. Brum WS, Cullen NC, Janelidze S, et al. A two-step workflow based on plasma p-tau217 to screen for amyloid β positivity with further confirmatory testing only in uncertain cases. *Nature Aging*. 2023;3(9):1079–1090.
21. Mattsson-Carlgren N, Collij LE, Stomrud E, et al. Plasma Biomarker Strategy for Selecting Patients With Alzheimer Disease for Antiamyloid Immunotherapies. *JAMA Neurology*. 2024;81(1)
22. Braak H, Thal DR, Ghebremedhin E, Del Tredici K. Stages of the pathologic process in Alzheimer disease: age categories from 1 to 100 years. *J Neuropathol Exp Neurol*. Nov 2011;70(11):960–9. doi:10.1097/NEN.0b013e318232a379
23. Jack CR, Jr., Knopman DS, Jagust WJ, et al. Tracking pathophysiological processes in Alzheimer's disease: an updated hypothetical model of dynamic biomarkers. *Lancet Neurol*. Feb 2013;12(2):207–16. doi:10.1016/S1474-4422(12)70291-0
24. Jack CR, Andrews JS, Beach TG, et al. Revised criteria for diagnosis and staging of Alzheimer's disease: Alzheimer's Association Workgroup. *Alzheimer's & Dementia*. Aug 2024;20(8):5143–5169.
25. Leuzy A, Mattsson-Carlgren N, Palmqvist S, Janelidze S, Dage JL, Hansson O. Blood-based biomarkers for Alzheimer's disease. *EMBO molecular medicine*. 2022;14(1):EMMM202114408.
26. Salloway S, Chalkias S, Barkhof F, et al. Amyloid-related imaging abnormalities in 2 phase 3 studies evaluating aducanumab in patients with early Alzheimer disease. *JAMA Neurology*. 2022;79(1):13–21.
27. Cummings JL, Zhou Y, Lee G, et al. Alzheimer's disease drug development pipeline:

2025. *Alzheimer's & Dementia: Translational Research & Clinical Interventions*. 2025;11(2):e70098.
28. Cummings J, Zhou Y, Lee G, Zhong K, Fonseca J, Cheng F. Alzheimer's disease drug development pipeline: 2024. *Alzheimer's & Dementia: Translational Research & Clinical Interventions*. 2024;10(2):e12465.
29. Chen S, Cao Z, Nandi A, et al. The global macroeconomic burden of Alzheimer's disease and other dementias: estimates and projections for 152 countries or territories. *The Lancet Global Health*. 2024;12(9):e1534–e1543.
30. Rabinovici GD, Gatsonis C, Apgar C, et al. Association of amyloid positron emission tomography with subsequent change in clinical management among medicare beneficiaries with mild cognitive impairment or dementia. *JAMA*. 2019;321(13):1286–1294.
31. Mattke S, Cho SK, Bittner T, Hlávka J, Hanson M. Blood-based biomarkers for Alzheimer's pathology and the diagnostic process for a disease-modifying treatment: projecting the impact on the cost and wait times. *Alzheimer's & Dementia: Diagnosis, Assessment & Disease Monitoring*. 2020;12(1):e12081.
32. Schindler SE, Karikari TK, Ashton NJ, et al. Effect of race on prediction of brain amyloidosis by plasma Aβ42/Aβ40, phosphorylated tau, and neurofilament light. *Neurology*. 2022;99(3):e245–e257.
33. Brickman AM, Manly JJ, Honig LS, et al. Plasma p-tau181, p-tau217, and other blood-based Alzheimer's disease biomarkers in a multi-ethnic, community study. *Alzheimer's & Dementia*. 2021;17(8):1353–1364.
34. Largent EA, Grill JD, O'Brien K, Wolk D, Harkins K, Karlawish J. Testing for Alzheimer disease biomarkers and disclosing results across the disease continuum. *Neurology*. 2023;100(21):1010–1019.
35. Sperling RA, Donohue MC, Raman R, et al. Trial of Solanezumab in Preclinical Alzheimer's Disease. *New Engl J Med*. 2023;389(12):1096–1107.
36. Petersen ME, Zhou Z, Hall JR, et al. Health and aging brain study–health disparities (HABS-HD) methods and partner characteristics. *Alzheimer's & Dementia: Translational Research & Clinical Interventions*. 2025;11(3):e70140.
37. Wei M, Zhang Y, Wang M, et al. Plasma biomarkers as core mediators in functional network abnormalities: Evidence from a two-cohort study. *Alzheimers Dement*. Apr 2025;21(4)
38. Landau SM, Harrison TM, Baker SL, et al. Positron emission tomography harmonization in the Alzheimer's Disease Neuroimaging Initiative: A scalable and rigorous approach to multisite amyloid and tau quantification. *Alzheimers Dement*. Jan 2025;21(1)
39. Salvadó G, Janelidze S, Bali D, et al. Plasma Phosphorylated Tau 217 to Identify Preclinical Alzheimer Disease. *JAMA Neurology*. 2025;82(11)doi:10.1001/jamaneurol.2025.3217

Table1. Characteristics of Study Participants

Characteristic	Cohort, No. (%)			
	A4 and LEARN (n = 1582)	**HABS-HD (n = 1208)**	**ADNI (n = 1068)**	**SILCODE (n = 190)**
Sex, n (%)				
Female	948 (60)	752 (62)	570 (53)	115 (61)
Male	634 (40)	456 (38)	498 (47)	75 (39)
Education, Mean (SD), y	16.62 (2.76)	14.34 (3.52)	16.40 (2.52)	13.40 (3.29)
Visit span, Median (IQR), y	4.66 (1.65 – 5.20)	0 (0 – 2.08)	0 (0 – 3)	0 (0 – 0)
Age at first visits, Mean (SD), y	71.7 (4.7)	69.2 (6.3)	74.0 (7.5)	69.4 (6.2)
Age at last visits, Mean (SD), y	74.6 (5.0)	69.6 (6.3)	75.0 (7.6)	69.9 (6.3)
Clinical Diagnosis at first visits, n (%)				
Cognitively unimpaired	1,570 (99)	912 (75)	605 (57)	156 (82)
Mild cognitive impairment	12 (0.8)	251 (21)	347 (32)	24 (13)
Dementia	0 (0)	45 (3.7)	116 (11)	10 (5.3)
Clinical Diagnosis at last visits, n (%)				
Cognitively unimpaired	1,213 (77)	902 (75)	591 (55)	156 (82)
Mild cognitive impairment	364 (23)	261 (22)	351 (33)	24 (13)
Dementia	5 (0.3)	45 (3.7)	126 (12)	10 (5.3)
Amyloid PET positivity at	974 (62)	310 (26)	478 (45)	72 (38)

Characteristic	Cohort, No. (%)			
	A4 and LEARN (n = 1582)	HABS-HD (n = 1208)	ADNI (n = 1068)	SILCODE (n = 190)
first visits, n (%)				
Amyloid PET positivity at last visits, n (%)	1,038 (66)	316 (26)	498 (47)	77 (41)
p-tau217 at first visits, Mean (SD), pg/mL	0.2 (0.1)	0.4 (0.3)	0.3 (0.3)	0.5 (0.4)
p-tau217 at last visits, Mean (SD), pg/mL	0.3 (0.1)	0.5 (0.3)	0.3 (0.3)	0.5 (0.4)

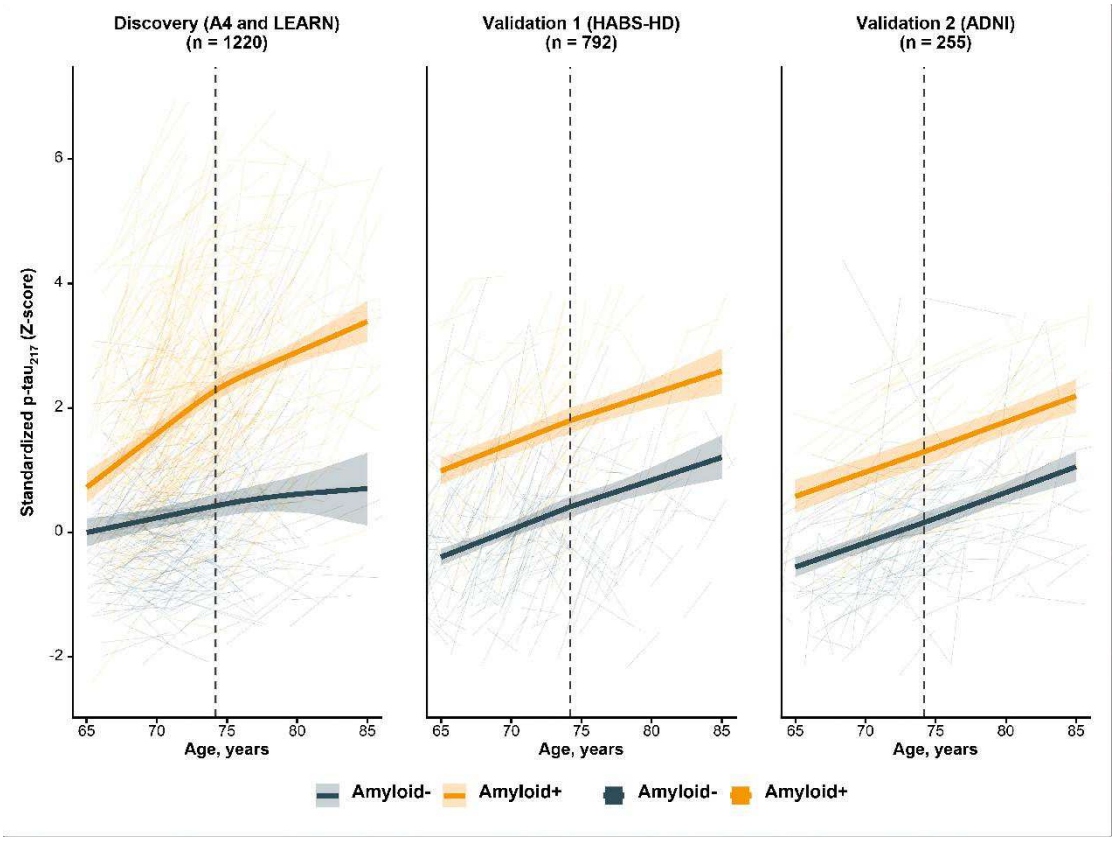

Figure 1 Longitudinal Trajectories of Standardized Plasma P-Tau 217 by Amyloid Status in CU Participants

Faint background lines represent individual longitudinal trajectories of standardized plasma P-tau217 z scores. Solid bold lines indicate the estimated population-level trajectories derived

from Bayesian mixed-effects models, with shaded regions representing 95% credible intervals. The vertical dashed line at age 74.45 years denotes the data-driven temporal inflection point identified in the discovery cohort (A4 and LEARN) and subsequently evaluated as a fixed knot in the 2 independent validation cohorts (HABS-HD and ADNI). Orange indicates Aβ–positive participants; dark blue indicates Aβ-negative participants.

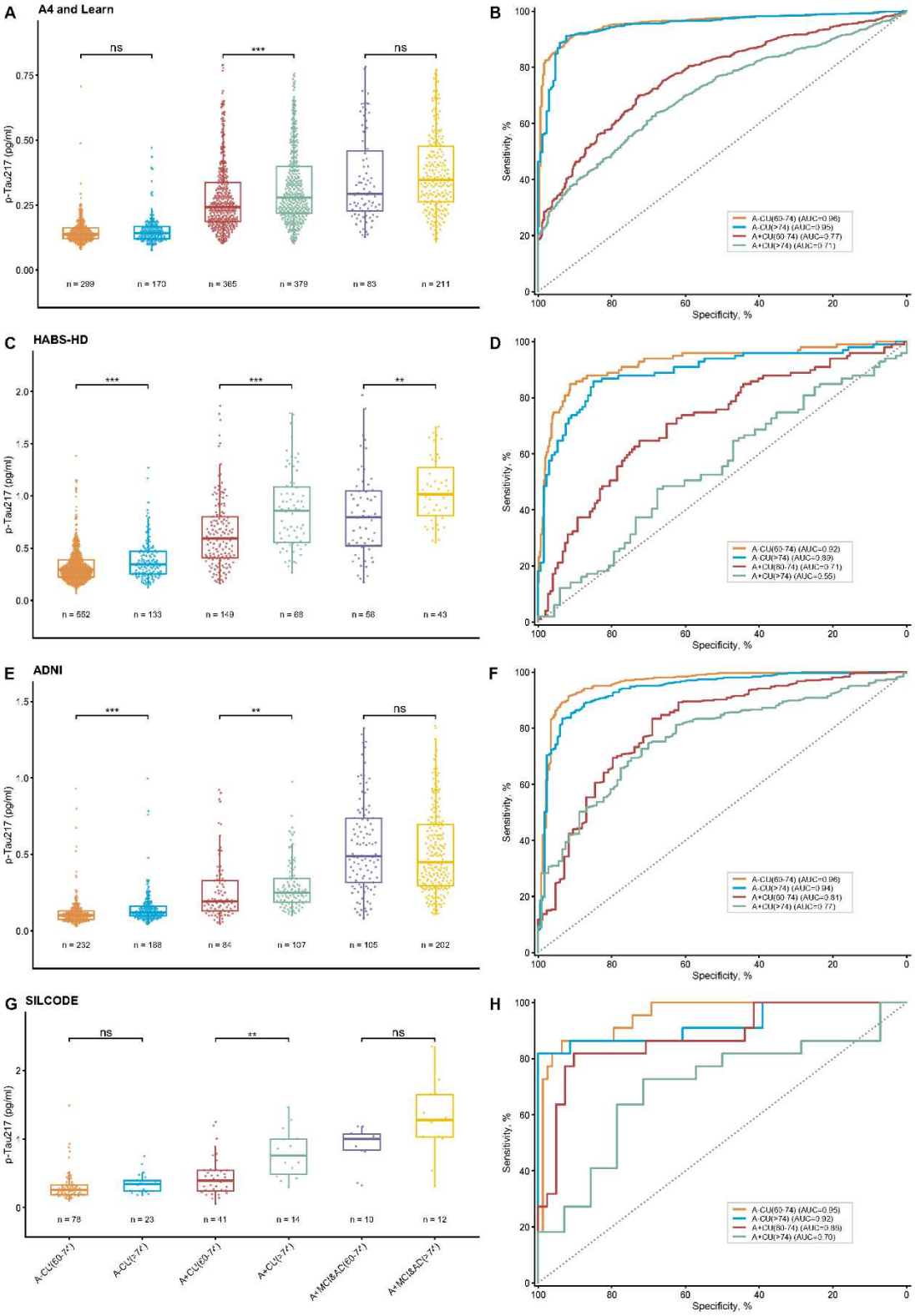

Figure2 Plasma P-Tau 217 Concentrations and Discriminative Accuracy Across Age and Clinical Subgroups

Panels A, C, E, and G display plasma p-tau217 concentrations stratified by Aβ status, clinical diagnosis, and age strata (60 to 74 years vs ≥74 years) across the 4 cohorts. The horizontal line

within each box indicates the median; the top and bottom of the box represent the 75th and 25th percentiles, respectively; and the whiskers extend to 1.5 times the interquartile range. Individual data points are overlaid. Asterisks indicate statistical significance from pairwise comparisons of log-transformed concentrations using analysis of covariance adjusted for sex and education level. Panels B, D, F, and H display ROC curves illustrating the ability of plasma p-tau217 to differentiate Aβ-positive symptomatic patients (MCI and dementia) from 4 distinct CU reference groups stratified by Aβ status and age. ns, not significant (** $P < .01$; *** $P < .001$).

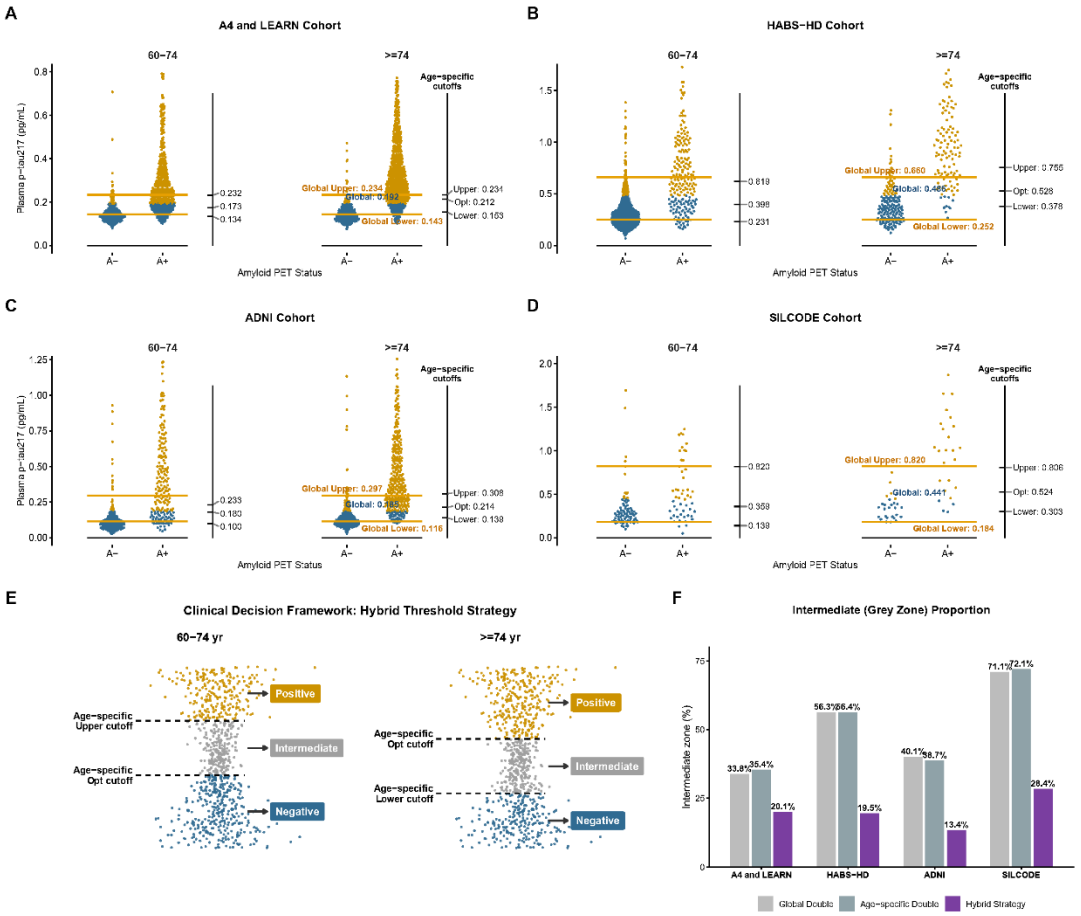

Figure3 Derivation of Plasma P-Tau 217 Diagnostic Thresholds and Implementation of the Age-stratified Hybrid Strategy

Panels A, B, C, and D illustrate the distribution of plasma p-tau217 concentrations stratified by Aβ PET status (A− vs A+) and age group (60 to 74 years vs ≥74 years) across the 4 cohorts. Data points represent individual participants and are color-coded based on the global optimal single cutoff (orange indicates concentrations at or above the cutoff; blue indicates concentrations below the cutoff). Solid orange horizontal lines represent the upper and lower bounds of the global double cutoffs. Age-specific cutoffs are annotated on the right y-axis, where Opt denotes the age-specific optimal single cutoff, and Upper and Lower denote the bounds of the age-specific double cutoffs. Panel E presents the conceptual clinical decision framework for the age-stratified hybrid threshold strategy. For adults aged 60 to 74 years, the intermediate zone is bounded by the age-specific optimal cutoff (lower bound) and the age-specific upper cutoff (upper bound). For adults aged 74 years and older, the indeterminate zone is bounded by the age-specific lower cutoff (lower bound) and the age-specific optimal cutoff (upper bound). Data points are color-coded to represent final classifications: positive (gold), intermediate (gray), and negative (blue). Panel F displays the proportion of participants classified into the intermediate zone using the standard global double cutoff (light gray bars),

strictly age-specific double cutoff (dark gray bars), and the proposed hybrid strategy (purple bars).

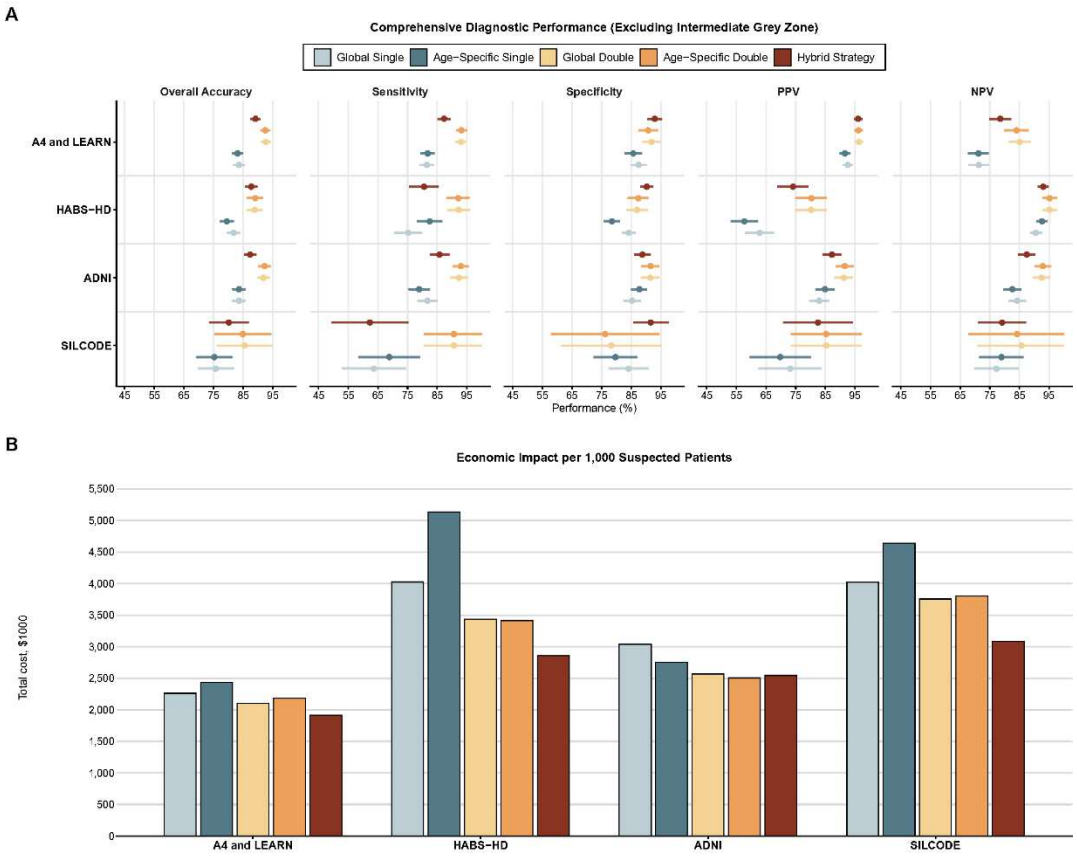

Figure4 Diagnostic Performance and Health Economic Impact of Plasma P-tau 217 Threshold Strategies

Panel A displays comprehensive diagnostic performance metrics, including overall accuracy, sensitivity, specificity, PPV, and NPV, across the 4 evaluated cohorts. Data points represent percentage estimates, and horizontal error bars indicate 95% confidence intervals. Participants classified into the intermediate zone were excluded from these diagnostic performance calculations. Panel B illustrates the estimated total diagnostic and misclassification costs per 1000 suspected patients for each cohort. Total costs incorporate the financial penalties associated with false-positive classifications, false-negative classifications, and the requirement for confirmatory PET for indeterminate cases. In both panels, colors denote the 5 diagnostic strategies: standard global single cutoff (light blue), strictly age-specific single cutoff (slate blue), standard global double cutoff (pale yellow), strictly age-specific double cutoff (orange), and the proposed age-stratified hybrid strategy (dark red).

Supplementary Files

This is a list of supplementary files associated with this preprint. Click to download.

- Supplementary2.docx
- Supplementary1.docx